Silver Mediation of Fe(VI) Charge Transfer: Activation of the K_2FeO_4 Super-iron Cathode

Stuart Licht,* Vera Naschitz, and Susanta Ghosh

Department of Chemistry and Institute of Catalysis Science, Technion - Israel Institute of Technology, Haifa, 32000, Israel

Received: December 31, 2001; In Final Form: March 29, 2002

An unexpectedly large Ag(II) mediation of Fe(VI) redox chemistry improves alkaline Fe(VI) cathodic charge transfer. Combined with a Zn anode, this results in a cell with 3- to 5-fold higher energy capacity than the conventional high-power Zn/MnO_2 alkaline battery, and twice that previously observed for $Zn/BaFeO_4$. Both experimental results and a model of this phenomenon are presented. The Ag(II) salt may be introduced as a simple composite of AgO with the Fe(VI) salt. The Fe(VI) super-iron salt K_2FeO_4 has a high $3e^-$ intrinsic charge capacity (406 mA/g), and is more environmentally benign than the Fe(VI) salt $BaFeO_4$, but had exhibited comparatively poor charge transfer. Successful AgO cathodic activation of both K_2FeO_4 and $BaFeO_4$ redox chemistry are presented. Various other K_2FeO_4 activators are also studied. An observed interaction of Fe(VI) with Mn(VII/VI) can improve charge efficiency of a K_2FeO_4 composite with $KMnO_4$ or $BaMnO_4$, albeit not to the extent observed in an K_2FeO_4/AgO composite cathode. The extent of an activation effect of oxides, hydroxides, and titanates salts, as well as $KMnO_4$, $BaMnO_4$, $AgMnO_4$, and fluorinated graphites, on the cathodic discharge of K_2FeO_4 are probed.

1. Introduction

Recently we introduced a series of battery types, based on an unusual Fe(VI) cathodic charge storage.[1] Iron typically occurs as a metal or in the valence states Fe(II) or Fe(III). Fe(VI) species have been known for over a century, although its chemistry remains relatively unexplored.[2] By the mid 20th century, even comprehensive texts such as Cotton & Wilkinson's *Inorganic Chemistry* no longer mention +6 valence iron, although more recently highly oxidized irons have been explored as an alternate oxidant for synthesis,[2] and for chlorination purification of water,[3] and as intermediate in biological charge-transfer processes.[4] The term "ferrate" has been variously applied to both Fe(II) and Fe(III) compounds. Instead, due to their highly oxidized iron basis, multiple electron transfer, and high intrinsic energy, we refer to cells containing iron compounds in a greater than three valence state as "super-iron" batteries. The charge insertion or reduction of Fe(VI) represents an energetic and high-capacity source of cathodic charge.

We have synthesized, characterized, and compared several Fe(VI) compounds to introduce and study their functionality for primary, secondary, and nonaqueous electrochemical energy storage.[1,5−14,22,23] An alkaline battery cathode based on $BaFeO_4$ contains intrinsic iron in the valence state Fe(VI) and exhibits a facile, high-potential $3e^-$ reduction. The cathodic discharge potential of alkaline Fe(VI) reduction is 0.25 V favorable to that of MnO_2, and the intrinsic 3 F/mole charge capacity of Fe(VI) salts such as K_2FeO_4 of 406 mA g^{-1} and $BaFeO_4$ of 313 mA g^{-1} compares favorably with the 1 F/mole charge capacity of the conventional MnO_2 cathode.

In the high-power discharge domain the $BaFeO_4$ cathode provides over a 2-fold increase in storage capacity compared to the conventional alkaline MnO_2 cathode.[1] Two of the main challenges to the implementation of the $BaFeO_4$ cathode are its stability and environmental impact. The stability of $BaFeO_4$ is less than that for K_2FeO_4 (which degrades by less than 0.1% per year).[10,11] Furthermore, K_2FeO_4 salts will not generate the regulatory issues that can arise for $BaFeO_4$ (recently, as a general class barium salts have been restricted by the U.S. EPA).[15] Yet, compared to $BaFeO_4$, cathodic charge transfer to pure K_2FeO_4 is considerably less efficient, and only a small fraction of the intrinsic $3e^-$ capacity is generated at high discharge rates.[1,5−7,10,12,14] $SrFeO_4$ was observed to sustain cathodic current densities intermediate to those of K_2FeO_4 and $BaFeO_4$.[8]

An electrochemical storage based on a zinc anode, an aqueous electrolyte, and a manganese dioxide cathode has been a dominant primary battery chemistry for over a century. The Zn/MnO_2 cell remains one of the most widely distributed products in the world and the most widely used consumer battery. This is despite its low intrinsic energy capacity and a particularly low practical energy capacity in high power applications, which is insufficient for developing electronic, lighting, and medical devices. Energy, power, mass, safety, and cost of this electrochemical system are constrained by its MnO_2 cathode.

In this study a co-cathode redox and electronic mediation which can enhance Fe(VI) charge transfer is modeled and demonstrated with AgO activation of the K_2FeO_4 cathode. A substantial increase in electrochemical energy storage is reported, resulting in an additional 2-fold increase in high-power discharge storage capacity.

2. Experimental Section

Preparation and analysis of K_2FeO_4 and $BaFeO_4$ have been recently detailed elsewhere.[10,11] K_2FeO_4 of 97−98.5% is prepared according to

$$Fe(NO_3)_3{\cdot}9H_2O + 3/2KClO + 5KOH \rightarrow K_2FeO_4 + 3/2KCl + 3KNO_3 + 23/2H_2O \quad (1)$$

* Corresponding author. E-mail: chrlicht@techunix.technion.ac.il. URL: http://www.technion.ac.il/technion/chemistry/staff/licht/

10.1021/jp014720j CCC: $22.00
Published on Web 05/21/2002

The dried K_2FeO_4 product has been found to be stable in time on the order of years and may be used for $BaFeO_4$ synthesis directly or after storage. In this synthesis, dissolved $Ba(OH)_2 \cdot 8H_2O$ is mixed with a solution of dissolved K_2FeO_4 precipitating $BaFeO_4$ as previously described, yielding 96−98% purity $BaFeO_4$, according to[10,11]

$$K_2FeO_4 + Ba(OH)_2 \rightarrow BaFeO_4 + 2KOH \qquad (2)$$

AgO is prepared by standard methods (the reaction at 85 °C of an alkaline $AgNO_3$ solution with $K_2S_2O_8$) in accord with

$$4AgNO_3 + 2K_2S_2O_8 + 8NaOH \rightarrow 4AgO + K_2SO_4 + 3Na_2SO_4 + 2NaNO_3 + 2KNO_3 + 4H_2O \qquad (3)$$

This study probes cathodic charge transfer through galvanostatic three-electrode measurements (utilizing a Pine Instruments AFCBP1 bipotentiostat in the constant current mode, with a Ag/AgCl reference electrode), as well as the preparation and use of two-electrode sealed cylindrical alkaline cells. Although not isolating the cathode redox couple as effectively as in a galvanostatic or potentiostatic three-electrode configuration, this two-electrode configuration has several advantages; the same type of anode was used throughout the study (as removed from the commercial Zn alkaline cell). As this anode exhibits facile (low polarization, efficient) oxidation, the charge-transfer attributes of the cathode are effectively demonstrated. It is the cathode that limits the observed discharge characteristics of these cells. Advantages of this two-electrode cell are its reproducibility, sealing (preventing competing oxygen reduction effects), and that the cell requires a minimum of electrolyte and provides a direct comparison to a widely distributed commercial cell. Components are removed from standard commercial AAA alkaline cells (a cylindrical cell configuration with diameter 10.1 mm and a 42 mm cathode current collector case height), and the outer MnO_2 mix is replaced with any cathode mix used in these experiments, followed by reinsertion of the separator, Zn anode mix, gasket, and anode collector and resealing of the cell. The cathode composites contain various cathode salts, 1 μm graphite (Leico Industries), and 13.5 M KOH electrolyte added to support the cathode reduction. Cell potential variation over time was measured via LabView Data Acquisition on a PC, and cumulative discharge, as ampere hours, was determined by subsequent integration.

3. Results and Discussion

3.1. Inhibition of Fe(VI) Charge Transfer. The alkaline galvanostatic reduction of solution phase Fe(VI) on Pt generates an observable solid Fe(III) overlayer and sustains cathodic current densities of only less than 100 μA cm^{-2}. As seen in comparison in Figure 1, solid Fe(VI) cathodes can sustain 2 orders of magnitude higher current density, highest when mixed with several percent of graphite. As represented in the scheme included within the figure, Fe(VI) charge transfer inhibition, when occurring, appears directly related to buildup of a low conductivity Fe(III) reduction product at the Fe(VI)/cathode current collector interface. We have used FTIR, ICP, and X-ray powder diffraction to study the Fe(III) products.[11] From the FTIR, these Fe(VI) discharge products contain hydroxide and Fe(III) salts, but the amorphous nature of the observed spectra does not lead to identification of the specific $M_dFe(III)O_x(OH)_y(H_2O)_z$ product (M = K_2 or Ba). It is reasonable to assume that the product will vary with pH, the extent of hydration, and the degree of Fe(VI) discharge; coexisting product stoichiometries may include

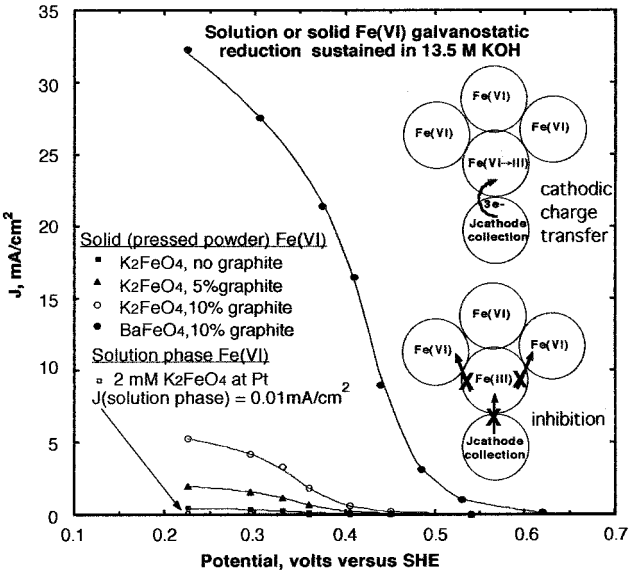

Figure 1. Galvanostatic reduction on Pt for 2 mM K_2FeO_4 in 13.5 M KOH or the indicated pressed Fe(VI) powders on Pt in 13.5 M KOH. Galvanostatic reduction is measured as the current density sustained at various potentials versus an Ag/AgCl reference electrode and shifted by 0.2 V to the standard hydrogen electrode potential, SHE.

$$Fe_2O_3 + xH_2O \rightleftarrows 2FeOOH\cdot(x-1)/2H_2O \qquad (4)$$

$$Fe_2O_3 + xBa(OH)_2 \rightleftarrows Ba_xFe_2O_{(3+x)}\cdot yH_2O + (x-y)H_2O \qquad (5)$$

$$Fe_2O_3 + 2xKOH \rightleftarrows K_{2x}Fe_2O_{(3+x)}\cdot yH_2O + (x-y)H_2O \qquad (6)$$

It is evident from the observed higher relative Coulombic efficiencies of $BaFeO_4$ cathodes,[1,5−7,10,12,14] and from the high current densities sustained in Figure 1, that the barium product of a $BaFeO_4$ reduction does not inhibit charge transfer to the degree of inhibition of the potassium product of K_2FeO_4 reduction.

K_2FeO_4 and $BaFeO_4$ permanganate (as in $KMnO_4$) and manganate (as in K_2MnO_4) exhibit energetically similar alkaline rest potentials, which in functioning cells may exhibit a Nernstian shift of over 0.1 V, depending on the relative activities of the cell constituents. The conventional MnO_2 cathode exhibits an alkaline rest potential approximately 250 mV lower.

$$FeO_4^{2-} + 5/2H_2O + 3e^- \rightarrow 1/2Fe_2O_3 + 5OH^- \qquad E = 0.6 \text{ V vs SHE} \qquad (7)$$

$$MnO_4^- + e^- \rightarrow MnO_4^{2-} \qquad E = 0.6 \text{ V vs SHE} \qquad (8)$$

$$MnO_4^{2-} + 2H_2O + 2e^- \rightarrow MnO_2 + 4OH^- \qquad E = 0.6 \text{ V vs SHE} \qquad (9)$$

$$MnO_2 + 1/2H_2O + e^- \rightarrow 1/2Mn_2O_3 + OH^- \qquad E = \sim 0.35 \text{ V vs SHE} \qquad (10)$$

3.2. Chemical Mediation of Fe(VI) Charge Transfer. In a recent letter to this journal, we observed a permanganate, Mn(VII), improvement of (both potassium and barium) Fe(VI) charge transfer.[14] In Figure 2 we propose a mechanism consistent with this facile charge transfer. With a similar alkaline potential, an analogous description for a manganate, Mn(VI),

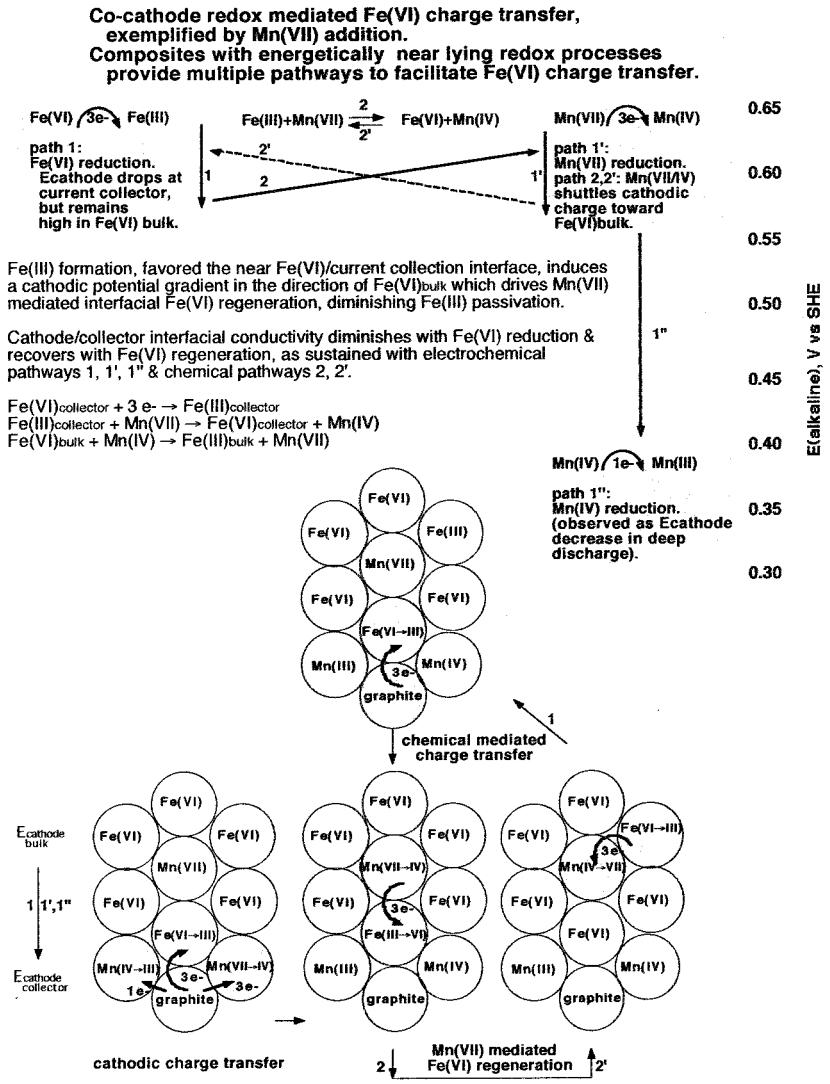

Figure 2. Co-cathode redox mediated Fe(VI) charge transfer, exemplified by Mn(VII) addition. Composites with near lying redox processes provide multiple pathways to facilitate Fe(VI) charge transfer; illustrated here by energy, mechanism, and chemical schematic representation.

facilitated Fe(VI) process will be evident from eq 12, but is not included in the Figure 2 description for clarity. The process utilizes the overlapping energetics of Mn(VII) and Fe(VI) redox chemistry to provide alternate pathways to minimize the effect summarized in Figure 1 of Fe(III) charged transfer inhibition and promoting Fe(VI) regeneration. The driving force for the Fe(VI) regeneration is the chemical and potential gradient that will spontaneously arise as the cathode discharges and, which as described in Figure 2, creates an anodic shift in more highly reduced portions of the cathode. Fe(III) at these sites is spontaneously regenerated to nonpassiviating Fe(VI) by Mn-(VII), as expressed by

$$2MnO_4^- + Fe_2O_3 + 2OH^- \rightleftarrows 2MnO_2 + 2FeO_4^{2-} + H_2O \quad (11)$$

(or via manganate as expressed by)

$$3MnO_4^{2-} + H_2O + Fe_2O_3 \rightleftarrows 3MnO_2 + 2OH^- + 2FeO_4^{2-} \quad (12)$$

This same potential gradient will will drive Mn(IV) regeneration to Mn(VII) via interior (bulk) Fe(VI) and the reverse reaction described in eq 11. This provides a charge shuttle to access bulk Fe(VI), which is only possible due to the near lying redox potentials of the Fe(VI/III) and Mn(VII/IV) half reactions. As detailed in Figure 2, the process may be summarized by the co-cathode chemical mediation of the Fe(VI/III) redox reaction to prevent Fe(VI) depletion near the cathode current collector and provide facile charge-transfer according to

$$Fe(VI)_{collector} + 3e^- \rightarrow Fe(III)_{collector} \quad (13)$$

$$Fe(III)_{collector} + Mn(VII) \rightarrow Fe(VI)_{collector} + Mn(IV) \quad (14)$$

$$Fe(VI)_{bulk} + Mn(IV) \rightarrow Fe(III)_{bulk} + Mn(VII) \quad (15)$$

3.3. Chemical and Electronic Mediation of Fe(VI) Charge Transfer. The multiple pathway charge transfer model proposed in Figure 2 for chemically mediated facile Fe(VI) charge transfer is consistent with the improvement in charge collection and current density observed in the presence of permanganate co-cathodes and can be further probed by future impedance and chronopotentiostatic and galvanostatic measurements. For this study, the immediate specific significance is that refinement of the process also indicates means for further enhancements of Fe(VI) cathodic charge which are presented here. Again the proposed process observes that the low cathodic efficiency and current densities sustainable for an unmodified K_2FeO_4/graphite cathode are related to Fe(VI) depletion and the concurrent

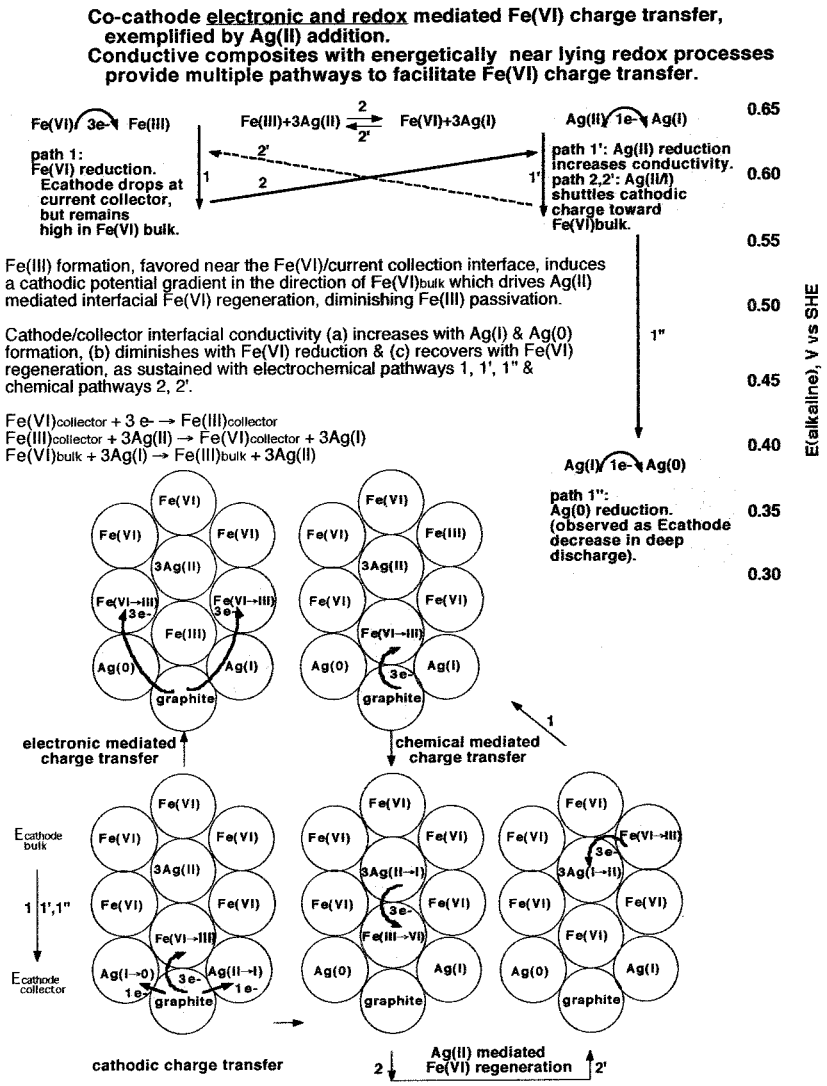

Figure 3. Co-cathode electronic and redox mediated Fe(VI) charge transfer, exemplified by Ag(II) addition. Composites with near lying redox processes provide multiple pathways to facilitate Fe(VI) charge transfer; illustrated here by energy, mechanism, and chemical schematic representation.

localized buildup of less conductive Fe(III). Also again the proposed process stipulates that an energetically similar co-cathode can alleviate this by spontaneous regeneration of this Fe(III). In addition, we now stipulate that the co-cathode also has sufficient electronic conduction to provide a parallel conductive matrix which further enhances Fe(VI) charge transfer.

The refined Figure 2 model is detailed in Figure 3 in a process for co-cathode *electronic and redox* mediated Fe(VI) charge transfer in which conductive composites with energetically near lying redox processes provide multiple pathways to facilitate Fe(VI) charge transfer. In Figure 3, the process is exemplifed by addition of an Ag(II) salt, in which the cathode/collector interfacial conductivity (a) increases with Ag(I) and Ag(0) formation, (b) diminishes with Fe(VI) reduction, and (c) recovers with Fe(VI) regeneration. An Ag(II) salt, such as AgO, as an Fe(VI) co-cathode is analogous to Mn(VII) and Mn(VI) in that it exhibits intrinsic two separate alkaline cathodic redox couples in the same potential domain as the single $3e^-$ Fe(VI) redox couple described in eq 7:

$$AgO + 1/2H_2O + e^- \rightarrow 1/2Ag_2O + OH \qquad E = 0.6 \text{ V vs SHE} \quad (16)$$

$$1/2Ag_2O + 1/2H_2O + e^- \rightarrow Ag + OH^- \qquad E = \sim 0.35 \text{ V vs SHE} \quad (17)$$

In comparison to Figure 2, in Figure 3 the additional pathway for Fe(VI) charge transfer is evident in the mid-left chemical schematic labeled electronic mediated charge transfer. Concurrent with increasing cathode consumption is an increasing buildup of conductive Ag, providing electronic access to bulk Fe(VI). Silver is a superlative metallic conductor; as the AgO discharges, the concentration of reduced silver grows and provides a growing conductive matrix to increasingly facilitate the Fe(VI) reduction.

3.4. Mn Mediation of Fe(VI) Charge Transfer. Supporting experimental evidence for the manganese (chemical) mediated Fe(VI) charge transfer has been detailed elsewhere.[14] This synergistic improvement of a K_2FeO_4 cathode with either $KMnO_4$ or $BaMnO_4$ is presented in Table 1. In the table it is seen that a pure K_2FeO_4 exhibits poor charge-transfer kinetics compared to a $BaFeO_4$ cathode at both low and high rate. These constant load discharges are respectively equivalent to constant current discharges of approximately 1.5 and 35 mA cm^{-2}. At low rate, the K_2FeO_4 discharges to a Coulombic efficiency, $\eta_{\text{efficiency}}$, of only 35% of the intrinsic $3e^-$ charge storage capacity, compared to $\eta_{\text{efficiency}}(BaFeO_4) = 85\%$ under the same discharge conditions. In this determination, the intrinsic capacities again calculated from the active cathode mass, assuming a 3 F $mole^{-1}$ Fe(VI → III) reduction, and subsequently compared

TABLE 1: Comparison of the Discharge Behavior in an Alkaline AAA Cell of Either a Pure K_2FeO_4 with a $BaFeO_4$ or a $BaMnO_4$ Cathode, or 50% Composite Cathodes with $KMnO_4$ or $BaMnO_4$[a]

dry cathode composition		measured storage capacity, discharged to 0.8 V cutoff					
		high rate (2.8 Ω load)			low rate (75 Ω load)		
wt % Fe salt	wt % Mn salt	charge (Ah)	$\eta_{efficiency}$	energy (Wh)	charge (Ah)	$\eta_{efficiency}$	energy (Wh)
100% $BaFeO_4$		0.67	51%	0.88	1.11	85%	1.78
	100% $BaMnO_4$	0.29	23%	0.34	0.80	62%	0.96
100% K_2FeO_4		0.24	17%	0.28	0.50	35%	0.68
50% K_2FeO_4	50% $KMnO_4$	0.41	22%	0.47	0.98	52%	1.41
50% K_2FeO_4	50% $BaMnO_4$	0.56	41%	0.67	0.85	62%	1.20

[a] The Coulombic efficiency, $\eta_{efficiency}$, is determined by normalizing the measured charge by the theoretical capacity (based on intrinsic charge equivalents in the cathode mass). The 100% cathodes contain either 4.2 g $BaFeO_4$, 4.1 g $BaMnO_4$, or 3.5 g K_2FeO_4. The solid cathode mix containing 50% $BaMnO_4$ has a mass of 3.8 g, while that containing 50% $KMnO_4$ has a mass of 3.5 g. In addition to the solid cathode mix indicated, the final cathode mix includes 9 wt % graphite and 9 wt % of 18 M KOH.

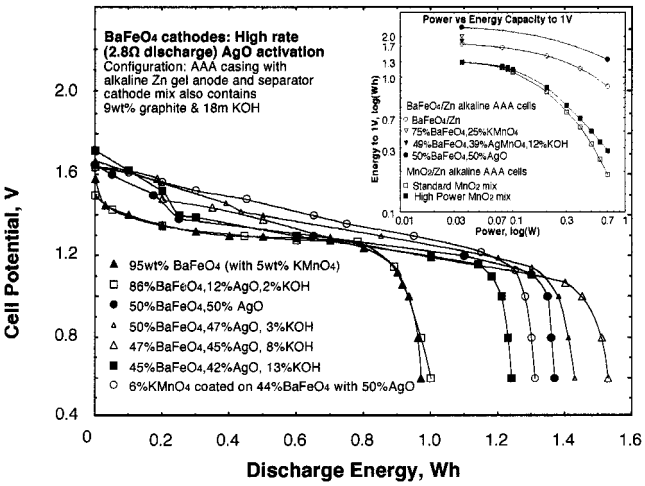

Figure 4. Cell potential and energy capacity of alkaline cells with $BaFeO_4$ cathode composites containing various weight fractions of AgO during discharge at a high constant load rate of 2.8 Ω. Cells use an alkaline AAA configuration including in the cathode 9 wt % graphite and 18 M KOH electrolyte. Inset: Energy at various powers during discharge of these and comparative cells.

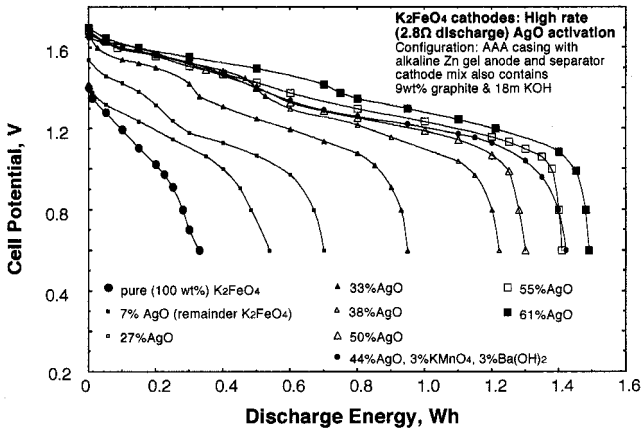

Figure 5. Cell potential and energy capacity of alkaline cells with K_2FeO_4 cathode composites containing various weight fractions of AgO during discharge at a high constant load rate of 2.8 Ω. Cells use an alkaline AAA configuration including in the cathode 9 wt % graphite and 18 M KOH electrolyte.

to the measured (Ah converted to F) discharged. High rates of charge transfer increase inhibition and under high rate conditions, the K_2FeO_4 discharges to a Coulombic efficiency of only 17%, and only one-third that observed for $\eta_{efficiency}(BaFeO_4)$ under the same conditions. At low rate, a 50 wt % composite cathode improves $\eta_{efficiency}(K_2FeO_4)$ from 35% to 52%, or 62%, respectively with either $KMnO_4$ or $BaMnO_4$, while at high rate $\eta_{efficiency}(K_2FeO_4)$ is improved from 17% to 22% or 41%. A better measure of the storage capability is the energy generated during discharge. As seen in the table, at high rate the $BaFeO_4$ cell exhibits a discharge energy of 0.88 Wh, compared to only 0.28 Wh for the K_2FeO_4 cell, which improves to 0.47 and 0.67 Wh, with respective addition of 50 wt % $KMnO_4$ or $BaMnO_4$.

3.5. Ag Mediation of Charge Transfer. The activation of $BaFeO_4$ and K_2FeO_4 by AgO in Figures 4 and 5 is substantial compared to that by $KMnO_4$ or $BaMnO_4$ observed in Table 1. As seen in Figure 5, as little as 7 wt % AgO composite with K_2FeO_4 yields a discharge energy comparable or larger than the 50 wt % the $KMnO_4/K_2FeO_4$ composite cathode. At larger AgO fractions, high rate discharge energies as great as 1.5 Wh are observed. In comparison with the top portion of Figure 6, it is seen that these discharge energies are substantially higher than conventional alkaline MnO_2 and are also higher than AgO (or $BaFeO_4$) alone.

Silver oxide cathodes, such as $Ag(I)_2O$, and silver peroxide, Ag(II)O, although costly, are characterized by attractive, relatively flat, discharge potential profiles, and in the case of AgO, a high intrinsic storage capacity compared to other active alkaline cathode materials. Consistent with their formula weight, the salts have respective 1 or 2 F $mole^{-1}$ capacities of 231 Ag_2O mAh g^{-1} and 433 mAh g^{-1} AgO. Yet as with MnO_2, AgO exhibits ineffective alkaline charge transfer at high discharge rate. Even in the presence of a significant conductive matrix, such as provided by the 9 wt % 1 μm graphite added to the cathode mix, the cathodes discharge respectively to only 35% or 37% of their intrinsic charge under 2.8 Ω load in an optimized AAA cell configuration and determined from the active cathode mass, assuming a 1 F $mole^{-1}$ Mn(IV → III) or a 2 F mol^{-1} Ag(II → 0) reduction. Due to the low cell discharge potential, the MnO_2 discharge capacity of 0.6 Wh observed in the top portion of Figure 6 diminishes by a further factor of 2 to 0.3 Wh, when the cell is discharged at a constant, higher power of 0.7 W. The constant 2.8 Ω load discharge capacity also falls to 0.4 Wh when 6 wt %, rather than 9 wt % of 1 μm graphite is utilized in the MnO_2 cathode.

In the top portion of Figure 6, the large intrinsic AgO capacity still results in a substantial measured energy capacity of 1.2 Wh despite the low AgO charge efficiency, although the high mass (over 5 g) of silver in the cell is generally a prohibitive cost factor. The Coulombic efficiency of Ag_2O is better ($\eta_{efficiency}(Ag_2O) = 46\%$) but yields a lower discharge energy of 0.9 Wh due to the lower 1 F mol^{-1} Ag(I) intrinsic capacity of Ag_2O, compared to AgO. Consistent with eqs 16 and 17, Ag_2O and AgO, exhibit distinct cathodic potentials in alkaline solution, and the expected single and double discharge voltage plateaus are observed in Figure 6 for the respective pure cathodes.

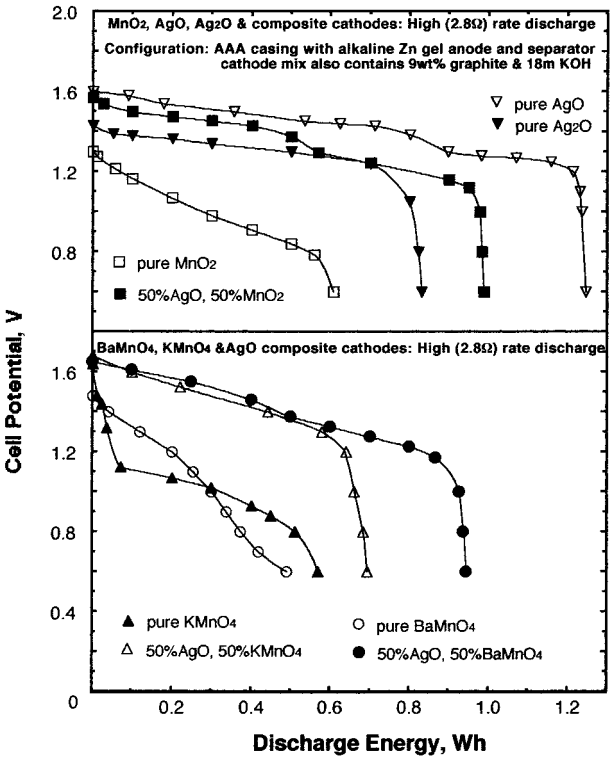

Figure 6. Cell potential and energy capacity of alkaline cells with either a pure 4.7 g MnO_2, 3.5 g $KMnO_4$, 4.1 g $BaMnO_4$, 6.0 g AgO, or 6.0 g Ag_2O cathode, or a composite cathode containing 50 wt % AgO with 50 wt % of either MnO_2, $KMnO_4$, $BaMnO_4$ during discharge at a high constant load rate of 2.8 Ω. Cells use an alkaline AAA configuration including in the cathode 9 wt % graphite and 18 M KOH electrolyte.

The lower portion of Figure 6 presents the ineffective discharge of a pure $KMnO_4$, Mn(VII), cathode. The generated 0.4 Wh reflects only 15% of the intrinsic 4 F mol^{-1} capacity of the $KMnO_4$ in the cathode. As also seen in the lower section of the figure, the pure $BaMnO_4$ (VI) cathode with a lower intrinsic 3 F mol^{-1} charge capacity discharged to a lower capacity than $KMnO_4$. Composite cathodes were also prepared containing both an Ag(II) salt and either MnO_2, $BaMnO_4$, or $KMnO_4$. Addition of 50 wt % AgO to each of the non-silver pure cathodes in Figure 6 leads to an improvement in the high rate cathodic charge generation, although each of these composite cathodes yields an energy capacity of less than 1.0 Wh, which is substantially less than that of the pure AgO cathode, and to a first approximation is the average of the separate cathode components.

Composite cathodes were also prepared containing both an Ag(II) salt and either K_2FeO_4 or $BaFeO_4$. Unlike MnO_2, $KMnO_4$, or $BaMnO_4$, the AgO has a synergistic activation on $BaFeO_4$ or K_2FeO_4 in which the combined discharge capacity of the composite Ag(II)/Fe(VI) cathode is larger than that of either cathode alone. A pure K_2FeO_4 cathode does not exhibit the high power density and Coulombic efficiencies evident in a $BaFeO_4$ cathode, although several factors (toxicity, availability, and intrinsic capacity) favor the K_2FeO_4 electrode. As seen comparing Figures 4 and 5, under comparable high load discharge conditions, in the absence of AgO, the $BaFeO_4$ cell generates 3-fold higher energy, and higher average power, compared to the K_2FeO_4 cell. Consistent with the observed flat discharge potential, a similar energy of 0.9 Wh is generated when the $BaFeO_4$ cell is discharged at either a constant 2.8 Ω (as shown) or a constant 0.5 A current, or discharged at a constant 0.7 W power (not shown).

As with K_2FeO_4, an unusually high energy discharge also occurs for an AgO cathode composite with the $BaFeO_4$ Fe(VI) salt. In Figure 4, a $BaFeO_4$/AgO cathode mix maintains the unusual high-power characteristic known for the $BaFeO_4$ cathode without AgO. Hence, the $BaFeO_4$ cathode both with and without AgO generates a power of at least 0.7 W over a constant 2.8 Ω load. However, in addition, the Fe(VI) composite cathode unexpectedly discharges for ∼170 min and generates 1.5 Wh, whereas under the same conditions, the $BaFeO_4$ cathode without AgO discharges for ∼80 to 90 min and generates 0.9 Wh. The $BaFeO_4$/AgO composite cathode exhibits a maximum discharge energy higher than either component alone. The discharge capacity is ∼5-fold higher than the equivalent constant power discharge of the conventional alkaline MnO_2 cell, or ∼3-fold higher than a constant resistive load discharge.

Compared to the $BaFeO_4$/AgO composite electrode effect, the activation of a K_2FeO_4 cathode by AgO is even more dramatic. The discharge time increase from ∼30 min to 150 min, and as seen in Figure 5, yields discharges in excess of 1.4 Wh. Incorporating a relatively low mass of added AgO, a K_2FeO_4 composite cathode, without other activators, will generate a significant alkaline energy discharge, and this low Ag amount is expected to further decrease upon introduction of additional alternate K_2FeO_4 activators. This study includes exploration of such alternate activators for K_2FeO_4, with and without added $KMnO_4$ and $BaMnO_4$.

3.6. Non-Ag Activation of K_2FeO_4. The K_2FeO_4 cathode can be improved by inclusion of various activators including manganese salts, although the observed magnitude of such effects is small compared to that in the AgO composite. Also a number of other composite K_2FeO_4 cathodes were explored without indications of charge-transfer activation. Hence, the AgO activation of K_2FeO_4 charge transfer is substantial and unexpected. When an alternate K_2FeO_4 activation with alternate composites did occur, it could be attributed to a nonmediative physical chemical phenomenon. Figure 7 summarizes the observed energy of the best of these alternative composites, which are further detailed in Tables 2 and 3.

As detailed in Table 2, added salts, such as LiOH, NaOH, or KOH do not increase a K_2FeO_4 cathode discharge, and the high rate discharge of K_2FeO_4 with and without 10% KOH is compared in the top section of Figure 7. Also included in Table 2 are relatively small, but significant, improvements of the K_2FeO_4 discharge energy with 10% addition of CsOH and $Ba(OH)_2$. We have investigated a related CsOH effect on a $BaFeO_4$ cathodic chemistry,[14] while the $Ba(OH)_2$ improvement is due to a partial conversion of K_2FeO_4 to the (facile charge transfer) barium salt in accord with eq 2. As also detailed in Table 2, a variety of added oxide, hydroxide, and salts do not increase a $BaMnO_4$ cathode's observed charge capacity. These include added KOH, LiOH, NaOH, $Ba(OH)_2$, $Sr(OH)_2$, $Ca(OH)_2$, $Mg(OH)_2$, Al_2O_3, $BaTiO_3$, or Co_2O_3. The addition of these possible activators is in lieu of the intrinsic storage capacity of the cathode. Hence as also seen in the table, if the activation effect is not substantial, then high additive levels (33 wt %) significantly diminish the observed energy capacity.

A composite K_2FeO_4/$BaMnO_4$ cathode yields a significantly higher energy capacity than either pure cathode. A pure $BaMnO_4$ cathode discharges to a significantly higher fraction of the intrinsic charge than does a $KMnO_4$ cathode,[14] although not approaching the high values observed for alkaline $BaFeO_4$ or MnO_2 cathodes. At low rate (75 Ω load/AAA configuration), the pure $BaMnO_4$ cathode cell yields (0.96 Wh) and an observed $V_{av} = 1.19$ V. As compared in Table 2, this manganate potential

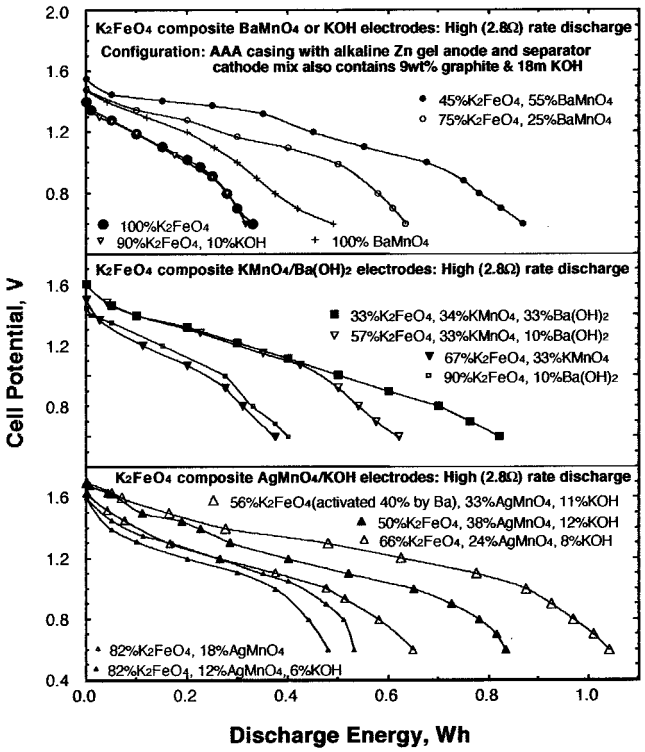

Figure 7. Cell potential and energy capacity of alkaline cells with K_2FeO_4 composite cathodes containing various relative amounts of $BaMnO_4$, $KMnO_4$, $AgMnO_4$, $Ba(OH)_2$, or KOH, compared to K_2FeO_4 in the cathode mix, during discharge at a high constant load rate of 2.8 Ω. In the composite cells, the combined mass of the K_2FeO_4 and other salts is intermediate to the mass of the pure salts (a pure cathode contains 3.5 g K_2FeO_4, 4.2 g $BaFeO_4$, 4.1 g $BaMnO_4$, 3.5 g $KMnO_4$, or 4.6 g $AgMnO_4$). Cells use an alkaline AAA configuration including 9 wt % graphite and 18 M KOH electrolyte in the cathode mix.

is considerably less than observed for the K_2FeO_4 cathode in Table 2, consistent with the manganate's greater fraction of the cathodic process constrained to the lower Mn(IV → III) potential of eq 10. However, the respective high and low rate discharge capacity of the pure K_2FeO_4 cathode, at 0.28 and 0.68 Wh, are somewhat lower than the capacities measured for the pure $BaMnO_4$ cathodes. As indicated in the top section of Figure 7 as the open or solid small circles, added barium manganate can significantly enhance the discharge energy of the K_2FeO_4 cathode. This is a synergistic effect, increasing the energy of either pure cathode alone. For the $K_2FeO_4/BaMnO_4$ composites, a maximum 2.8 Ω discharge energy of 0.78 Wh is measured for the cell containing 45 wt % K_2FeO_4 and 55 wt % $BaMnO_4$, which is more than double that seen for either the pure K_2FeO_4 or the pure $BaMnO_4$ cathode. As detailed in Table 3 at the low rate (constant 75 Ω load), the $K_2FeO_4/BaMnO_4$ composite cathode exhibits a nearly constant maximum energy capacity of 1.2 Wh over a wide composition range varying from 33%:67% to 67%:33%. KOH or Al_2O_3 added to $BaMnO_4$, impairs the discharge effectiveness both of the pure $BaMnO_4$ cathode (Table 2) and also of the $BaMnO_4/K_2FeO_4$ composite cathode (Table 3). $Ba(OH)_2$ added to $BaMnO_4$ also impairs the discharge effectiveness of the pure $BaMnO_4$ cathode, but modestly increases the discharge energy of the composite $BaMnO_4/K_2FeO_4$ cathode (Table 3) due to the improvements of $Ba(OH)_2$ on the pure K_2FeO_4 electrode (Table 2).

The discharge of $K_2FeO_4/KMnO_4$ composite cathodes was optimized with various additives. Consistently the $Ba(OH)_2$ was the most effective additive, and the high rate discharge is summarized in the midsection of Figure 7. In the presence of both Mn(VII) salts and Fe(VI), competing alkali earth hydroxide effects are complex. For example, in the reaction with $Ba(OH)_2$, the $KMnO_4$ reaction product is highly soluble (the product

TABLE 2: Comparison of the Discharge Behavior in an Alkaline AAA Cell of Either a K_2FeO_4, $KMnO_4$, or a $BaMnO_4$ Cathode with or without Added Hydroxide[a]

dry cathode composition, by mass						discharge to 0.8 V (constant load)			
						2.8 Ω		75 Ω	
Fe salt	wt %	Mn salt	wt %	salt	wt %	E (Wh)	V_{av} (V)	E (Wh)	V_{av} (V)
K_2FeO_4	100					0.28	1.17	0.68	1.36
K_2FeO_4	90			KOH	10	0.27	1.08	0.55	1.36
K_2FeO_4	90			$Ba(OH)_2$	10	0.35	1.15	0.79	1.44
K_2FeO_4	90			LiOH	10	0.30	1.09	0.63	1.31
K_2FeO_4	90			NaOH	10	0.24	1.05	0.60	1.35
K_2FeO_4	90			CsOH	10	0.34	1.17	0.83	1.44
		$BaMnO_4$	100			0.34	1.16	0.96	1.19
		$BaMnO_4$	90	KOH	10	0.32	1.10	0.98	1.18
		$BaMnO_4$	90	Al_2O_3	10	0.27	1.08	0.78	1.19
		$BaMnO_4$	90	$Ba(OH)_2$	10	0.29	1.11	0.76	1.20
		$BaMnO_4$	90	$Sr(OH)_2$	10	0.28	1.09	0.70	1.17
		$BaMnO_4$	90	$Ca(OH)_2$	10	0.29	1.07	0.73	1.18
		$BaMnO_4$	90	$Mg(OH)_2$	10	0.32	1.14	0.67	1.19
		$BaMnO_4$	90	LiOH	10	0.27	1.08	0.73	1.18
		$BaMnO_4$	90	NaOH	10	0.23	1.11	0.75	1.20
		$BaMnO_4$	90	$BaTiO_3$	10	0.28	1.08	0.93	1.16
		$BaMnO_4$	90	Co_2O_3	10	0.30	1.07	0.77	1.17
		$BaMnO_4$	67	KOH	33	0.22	1.10	0.50	1.19
		$BaMnO_4$	67	Al_2O_3	33	0.25	1.06	0.69	1.18
		$BaMnO_4$	67	$Ba(OH)_2$	33	0.15	1.07	0.49	1.14

[a] Relative amounts of the indicated solid cathode mix are presented. In addition, the final cathode mix includes 9 wt % graphite and 9 wt % of 18 M KOH. The LiOH salt cell gave similar results with a saturated LiOH electrolyte. The CsOH salt cell utilizes an 18 M CsOH electrolyte.

TABLE 3: Comparison of the Discharge Behavior in an Alkaline AAA Cell of a Cathode Composite Containing K_2FeO_4 and $BaMnO_4$ or K_2FeO_4 and $KMnO_4$[a]

dry cathode composition, by mass						discharge to 0.8 V (constant load)			
						2.8 Ω		75 Ω	
Fe salt	wt %	Mn salt	wt %	salt	wt %	E (Wh)	V_{av} (V)	E (Wh)	V_{av} (V)
K_2FeO_4	0	$BaMnO_4$	100			0.37	1.16	0.96	1.19
K_2FeO_4	5	$BaMnO_4$	95			0.44	1.16	1.03	1.26
K_2FeO_4	10	$BaMnO_4$	90			0.54	1.17	1.14	1.31
K_2FeO_4	25	$BaMnO_4$	75			0.59	1.17	1.16	1.39
K_2FeO_4	33	$BaMnO_4$	67			0.65	1.19	1.20	1.40
K_2FeO_4	45	$BaMnO_4$	55			0.78	1.20	1.20	1.41
K_2FeO_4	50	$BaMnO_4$	50			0.67	1.20	1.20	1.41
K_2FeO_4	67	$BaMnO_4$	33			0.66	1.20	1.19	1.44
K_2FeO_4	75	$BaMnO_4$	25			0.57	1.22	1.12	1.45
K_2FeO_4	90	$BaMnO_4$	10			0.38	1.21	0.98	1.45
K_2FeO_4	95	$BaMnO_4$	5			0.38	1.19	0.71	1.43
K_2FeO_4	100	$BaMnO_4$	0			0.28	1.17	0.68	1.36
K_2FeO_4	33	$BaMnO_4$	57	Al_2O_3	10	0.62	1.19	1.10	1.37
K_2FeO_4	57	$BaMnO_4$	33	Al_2O_3	10	0.56	1.17	1.13	1.43
K_2FeO_4	33	$BaMnO_4$	57	KOH	10	0.61	1.20	1.17	1.39
K_2FeO_4	50	$BaMnO_4$	25	KOH	25	0.52	1.24	0.96	1.43
K_2FeO_4	57	$BaMnO_4$	33	KOH	10	0.65	1.23	1.00	1.43
K_2FeO_4	10	$BaMnO_4$	57	$Ba(OH)_2$	33	0.44	1.26	0.68	1.28
K_2FeO_4	33	$BaMnO_4$	34	$Ba(OH)_2$	33	0.60	1.28	0.92	1.51
K_2FeO_4	33	$BaMnO_4$	57	$Ba(OH)_2$	10	0.81	1.27	1.17	1.41
K_2FeO_4	50	$BaMnO_4$	25	$Ba(OH)_2$	25	0.78	1.28	1.15	1.51
K_2FeO_4	57	$BaMnO_4$	33	$Ba(OH)_2$	10	0.81	1.29	1.21	1.46
K_2FeO_4	57	$BaMnO_4$	10	$Ba(OH)_2$	33	0.76	1.29	1.27	1.61
K_2FeO_4	57	$KMnO_4$	10	$Ba(OH)_2$	33	0.63	1.26	1.04	1.16

[a] The cathode mix also includes graphite and electrolyte.

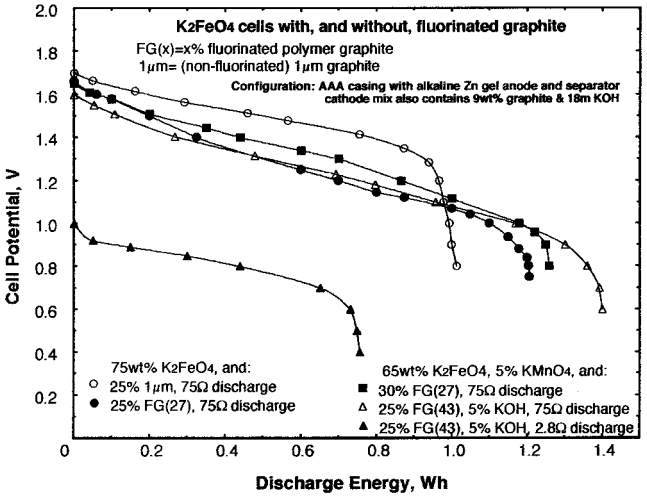

Figure 8. Cell potential and energy capacity of K_2FeO_4 cathode alkaline cells with various relative amounts, by weight, of regular or fluorinated graphite in the cathode mix, during discharge at the indicated load of either 2.8 Ω or 75 Ω. Cells use an alkaline AAA configuration including in the cathode 9 wt % graphite and 18 M KOH electrolyte.

$Ba(MnO_4)_2$ has an aqueous solubility of 18 molal). However, the alternative reaction K_2FeO_4 with $Ba(OH)_2$ forms $BaFeO_4$, which is insoluble in water. As seen in the midsection portion of Figure 3, the addition of $Ba(OH)_2$ to the $K_2FeO_4/KMnO_4$ cathode results in a significant increase in discharge energy, and at an average discharge potential greater than that observed for the $K_2FeO_4/KMnO_4$ composite without $Ba(OH)_2$. At both high and low rate, a maximum discharge energy is observed with the 33:57:10 wt % K_2FeO_4:$KMnO_4$:$Ba(OH)_2$ composition which provides 0.73 and 1.62 Wh respectively over either 2.8 Ω or 75 Ω load discharges.

$AgMnO_4$ provides an unusual salt in that the Ag valence acts in a manner intermediate to Ag(I) and Ag(II), that is as for $Ag(I + x)Mn(VII - x)O_4$, where $0 < x < 1$.[13,16] Of the permanganate and manganate salts explored to date, $AgMnO_4$ promotes one of the larger increases in the K_2FeO_4 alkaline cathode discharge, a phenomenon consistent with the observed Ag activation of Fe(VI), but the $AgMnO_4$ activation phenomenon is only substantial in the presence of KOH (added as a solid salt to the mix).[13] This is observed in the lowest section of Figure 7. In the absence of KOH, the 2.8 Ω discharge of the K_2FeO_4 cathode increases from to 0.3 Wh to ~0.4 Wh with addition of 18% $AgMnO_4$, but is enhanced to 0.5 Wh using only 12 wt % $AgMnO_4$ with KOH (6 wt %). This increases to ~0.8 Wh with inclusion of 38 wt % $AgMnO_4$ and 12 wt % KOH. Finally, as also seen in the figure, a K_2FeO_4, partially converted to the barium salt with a $Ba(OH)_2$ wash and mixed with $AgMnO_4$ and KOH, provides a cathode with a high rate discharge similar to the desired capacity of the $BaFeO_4$ cathode, exhibiting a higher energy capacity, but lower average discharge potential. Aspects of the interesting KOH activation of the pure $AgMnO_4$ alkaline cathode (without K_2FeO_4) are explored in a recent study,[13] and the $AgMnO_4$ activation of K_2FeO_4 is still lower than that observed in Figure 5 for the AgO mediation of K_2FeO_4 charge transfer.

The cathode reduction is supported by a conductive matrix provided through inclusion of graphite in the cathode mix. The K_2FeO_4 cathode can be enhanced by replacing a fraction of this active cathode material with a larger fraction of graphite to increase conductivity and thereby improve utilization of the remaining intrinsic Fe(VI → III) charge utilization. Hence in Figure 8, a 75 wt % K_2FeO_4 and 25 wt % graphite cathode mix yields a 75 Ω load discharge of 1.0 Wh, compared to 0.7 Wh for the comparable cell containing one-third the graphite. This effect is limited in that it also removes cathode active material from the cell. Recently, we have probed a series of fluorinated graphite materials that can serve not only as a conductive matrix but also which have an intrinsic cathodic capacity in alkaline media. Fluorinated graphite polymers of the form $(CF_x)_n$, which are also described by the weight percent of fluorine contained in the carbon, are prepared by the reaction of graphite or carbon materials under a variety of temperature and reaction conditions and have been widely studied as lithium intercalation electrodes.[17−21] As we have recently noted, and as presented in Figure 8 in this paper, replacement of the regular graphite fraction of the cathode mix with a fluorinated graphite can increase the aqueous alkaline cell capacity.[12] As additionally shown in this figure, further optimization of this cathode mix may be accomplished by variation of the degree of fluorination, and addition of hydroxide or permanganate. However, as evident in the figure, compared to nonfluorinated graphite, fluorinated graphite's relatively high resistance leads to a low voltage (and hence low power) discharge at a high rate, constant 2.8 Ω discharge.

3.7. Constant Power Comparison of MnO_2, $BaFeO_4$, and AgO/K_2FeO_4 Cathodes. The unusually high specific energy/specific power of various Fe(VI) alkaline batteries is summarized in the inset of Figure 4. Of relevance to both practical electronics and as a fundamental energy comparison, a constant power density, rather than constant load or constant current density, is a more stringent comparison of cathode capabilities. In this discharge the lower average cathode potential of the MnO_2 cathode (eq 10) compared to Fe(VI) (eq 7) must be compensated by a higher average current density, and this will further impair the MnO_2 charge transfer. As previously observed,[1] under conditions of constant, rapid 0.7 W discharge in an AAA cell configuration, the MnO_2 discharges to a maximum of 0.52 h (0.36 Wh), whereas a 5% $KMnO_4$/95% $BaFeO_4$ cathode (containing (4.0 g $BaFeO_4$) discharges for 1.26 h to 0.88 Wh.[11] Under the same conditions, for the composite AgO/K_2FeO_4 cathodes, a 8 wt % (0.3 g) AgO/92 wt % K_2FeO_4 cell discharges for 1.28 h to 0.90 Wh, a 20 wt % (0.7 g) AgO/80 wt % K_2FeO_4 cell discharges for 1.58 h to 1.11 Wh, and a 39 wt % (1.5 g) AgO/61 wt % K_2FeO_4 cell discharges for 2.13 h to 1.49 Wh.

4. Conclusion

An activated cathodic reduction is demonstrated for superiron cathodes, to increases the modest but expanding foundation of understanding of charge transfer of these unusual Fe(VI) charge storage salts. A model presented for co-cathode chemical and electronic mediation of Fe(VI) suggests charge transfer enhancement by Ag(II). This enhancement is experimentally observed in the form of AgO/K_2FeO_4 composite cathodes and provides a step toward an environmentally benign alkaline cathode with power and storage characteristics superior to the widely used conventional MnO_2 cathode. In a Zn anode alkaline cell, an AgO/K_2FeO_4 composite cathode provides a high rate discharge with 3- to 5-fold higher high power energy capacity (for example 1.5 Wh, compared to 0.36 Wh, at 0.7 W in a AAA cell configuration) than the conventional Zn/MnO_2 alkaline.

The chemical mediation of Fe(VI)/Mn(VII) or Fe(VI)/Mn(VI) can also improve charge of efficiency of both the composite $K_2FeO_4/KMnO_4$ or $K_2FeO_4/BaMnO_4$ cathodic discharge through inclusion of both salts in the cathode mix. The effect of oxide, hydroxides, titanates, fluorinated graphites, and $AgMnO_4$ on the cathodic process is also explored. In the absence of Ag(II)

activation, alkaline K_2FeO_4 AAA cells containing specific activators can improve the discharge energy and discharge behavior, approaching that previously observed for the $BaFeO_4$ cathode (0.88 Wh at high rate AAA discharge). Addition of 33% $KMnO_4$ and 10% $Ba(OH)_2$ to the pure K_2FeO_4 cathode mix increases the 2.8 Ω discharge 2-fold to 0.54 Wh. Alternatively, addition of 33% $BaMnO_4$ increases this to 0.58 Wh and to 0.81 Wh with 33% $BaMnO_4$ and 10% $Ba(OH)_2$. Compared to the pure K_2FeO_4 cathode, addition of 34% $AgMnO_4$ and 11% KOH increases the discharge energy to 0.78 Wh, which is further increased to 0.97 Wh when the K_2FeO_4 is pretreated with a $Ba(OH)_2$ wash.

Acknowledgment. We thank B. Wang, D. Rozen, and N. Halperin and M. Zuidman who participated in the analyses.

References and Notes

(1) Licht, S.; Wang, B.; Ghosh, S. *Science* **1999**, *285*, 1039.
(2) Johnson, M. D.; Read, J. F. *Inorg. Chem.* **1996**, *35*, 6795.
(3) Sharma, V. K.; Smith, J. O.; Millero, F. J. *Environ. Sci. Technol*. **1997**, *31*, 2486.
(4) Rryter, M.; Tyrell, R. M. *Free Radical Biol. Med.* **2000**, *28*, 289.
(5) Licht, S.; Wang, B.; Ghosh, S.; Li, J.; Naschitz, V. *Electrochem. Commun*. **1999**, *1*, 522.
(6) Licht, S.; Wang, B.; Ghosh, S.; Li, J.; Naschitz, V. *Electrochem. Commun*. **1999**, *1*, 527.
(7) Licht, S.; Wang, B.; Ghosh, S.; Tel-Vered, R.; Naschitz, V. *Electrochem. Commun*. **2000**, *2*, 535.
(8) Licht, S.; Naschitz, V.; Ghosh, S.; Lin, L.; Lui, B. *Electrochem. Commun*. **2001**, *3*, 340.
(9) Licht, S.; Wang, B. *Electrochem. Solid State Lett*. **2000**, *3*, 209.
(10) Licht, S.; Naschitz, V.; Liu, B.; Ghosh, S.; Halperin, N.; Halperin, L.; Rozen, D. *J. Power Sources* **2001**, *99*, 7.
(11) Licht, S.; Naschitz, V.; Lin. L.; Chen, J.; Ghosh, S.; Liu, B. *J. Power Sources* **2001**, *101/2*, 167.
(12) Licht, S.; Ghosh, S.; Dong, Q. *J. Electrochem. Soc.* **2001**, *148*, A1072.
(13) Licht, S.; Naschitz, V.; Liu, B.; Ghosh, S. *Electrochem Solid. State Lett*. **2001**, *4*, A209.
(14) Licht, S.; Ghosh, S.; Naschitz, V.; Halperin, N.; Halperin, L. *J. Phys. Chem. B* **2001**, *105*, 11933.
(15) *U.S. Federal Register* (January 3, 1997) Vol. B, No. 2, p 367.
(16) Mehne, L. F.; Wayland, B. B. *J. Inorg. Nucl. Chem*. **1975**, *37*, 1371.
(17) Nakajima, T.; Koh, M.; Gupta, V.; Zemva, B.; Lutar, K. *Electrochim. Acta* **2000**, *45*, 1655.
(18) Yazami, R.; Hany, P.; Masset, P.; Hamwi, A. *Mol. Cryst. Liq. Cryst. Sci. Technol*. **1998**, *310*, 397.
(19) Hamwi, A.; Al Saleh, I. *J. Power Sources* **1994**, *48*, 311.
(20) Bubyreva, N. S.; Mararenko, B.; Yu, K.; Pavlo, P.; Perederi, I. M.; Rozenblyum, N. D.; Tomin, O. A *Elektrokhimiya* **1982**, *18*, 1105.
(21) Watanabe, N. *Solid State Ionics* **1980**, *1*, 87.
(22) Licht, S.; Naschitz, V.; Wang, B. *J. Power Sources* **2002**, in press.
(23) Licht, S.; Ghosh, S. *J. Power Sources* **2002**, in press.